Resolution of phospholipid conformational heterogeneity in model membranes by spin-label EPR and frequency-domain fluorescence spectroscopy

ARTICLE *in* BIOPHYSICAL JOURNAL · APRIL 1991

Impact Factor: 3.97 · DOI: 10.1016/S0006-3495(91)82281-0 · Source: PubMed

Resolution of phospholipid conformational heterogeneity in model membranes by spin-label EPR and frequency-domain fluorescence spectroscopy

Thomas C. Squier,* James E. Mahaney,‡ J. J. Yin,§ Ching San Lai,§ and Joseph R. Lakowicz*

*Department of Biological Chemistry, University of Maryland, School of Medicine, Baltimore, Maryland 21201; ‡Department of Biochemistry, University of Minnesota Medical School, Minneapolis, Minnesota 55455; and §National Biomedical ESR Center, Department of Radiology, Medical College of Wisconsin, Milwaukee, Wisconsin 53226 USA

ABSTRACT We have utilized both fluorescent and nitroxide derivatives of stearic acid as probes of membrane structural heterogeneity in phospholipid vesicles under physiological conditions, as well as conditions of varying ionic strengths and temperatures where spectral heterogeneity has been previously observed and attributed to multiple ionization states of the probes. To identify the source of this spectral heterogeneity, we have utilized complimentary measurements of the relaxation properties (lifetimes) and motion of both (*a*) spin labeled and anthroyloxy derivatives of stearic acid (i.e., SASL and AS) and (*b*) a diphenylhexatriene derivative of phosphatidylcholine (DPH-PC) in single component membranes containing dimyristoylphosphatidylcholine (DMPC). We use an ^{15}N stearic-acid spin label for optimal sensitivity to membrane heterogeneity. The lifetime and dynamics of the fluorescent phospholipid analogue DPH-PC (with no ionizable groups over this pH range) were compared with those of AS, allowing us to discriminate between changes in membrane structure and the ionization of the label. The quantum yield and rotational dynamics of DPH-PC are independent of pH, indicating that changes in pH do not affect the conformation of the host phospholipids. However, both EPR spectra of SASL and the lifetime or dynamics of AS are affected profoundly by changes in solution pH. The apparent pK_a's of these two probes in DMPC membranes were determined to be near pH 6.3, implying that at physiological pH and ionic strength these stearic-acid labels exist predominantly as a single ionized population in membranes. Therefore, the observed temperature- and ionic-strength-dependent alterations in the spectra of SASL as well as the lifetime or dynamics of AS in DMPC membranes at neutral pH are due to changes in membrane structure rather than the ionization of the probes. The possibility that ionic gradients across biological membranes induce alterations in phospholipid structures, thereby modulating lipid-protein interactions is discussed.

INTRODUCTION

Spectroscopic analogues of membrane lipids have proven to be an important means of identifying the physical features of biological lipids that are relevant to modulating membrane function (reviewed by Marsh, 1981; Lai, 1982; Thomas, 1985; Lakowicz, 1988). While fluorescent or paramagnetic reporter groups attached covalently to phospholipids offer the advantage of being most analogous to the host lipid, derivatives of fatty acids often remain the spectroscopic probe of choice in the investigation of membrane dynamics due to the ease with which they are incorporated into both leaflets of biological membranes, their availability, and their long-term stability. In particular, spin labeled and anthroyloxy stearic acid derivatives have provided an important means of measuring the structural properties of the membrane and especially in quantitating the degree of membrane heterogeneity. As a result, the physical properties of these probes have received a considerable amount of attention. They appear to be randomly distributed in the plane of the bilayer, position themselves parallel to the membrane normal so that the α-carbonyl group is aligned with the head group region of the bilayer, and faithfully reflect the degree of orientational order and dynamics of the lipid molecules (Godici and Landsberger, 1974; Thulburn and Sawyer, 1978; Hauser et al., 1979; Taylor and Smith, 1981; Schachter et al., 1982; Eisinger and Flores, 1983; Lange et al., 1985; Bigelow and Thomas, 1987; Esmann et al., 1988; Squier and Thomas, 1989; Moser et al., 1989).

However, the possibility that these probes exist in multiple ionization states at neutral pH remains a problem that complicates the interpretation of spectral data taken under biological conditions and makes it difficult to determine if observed spectral heterogeneity results from (*a*) specific interactions between membrane components or from (*b*) multiple ionization states of the probe (which could be modulated by the ionic conditions under investigation). While the latter rationale has been

Abbreviations used in this paper: DMPC, dimyristoylphosphatidylcholine; SASL, stearic acid spin label; 2-AS, 2-(9-anthroyloxy)stearic acid; DPH-PC, 2-3-(diphenylhexatrienyl)-3-palmitoyl-L-α-phosphatidylcholine; EPR, electron paramagnetic resonance; SR-EPR, saturation-recovery EPR; T'_0, the apparent isotropic hyperfine splitting constant; $T'_\parallel$ and $T'_\perp$, the measured outer and inner splitting (in Gauss) resolved in the EPR spectrum.

Address correspondence to Thomas C. Squier, Dept. Biochemistry, University of Kansas, Lawrence, KS 66045-2106.

0006-3495/91/03/654/16 $2.00

used to explain the observation of multicomponent spectra for ^{14}N-5-SASL (near 50°C; 0.1 M phosphate buffer) at neutral pH in phosphatidylcholine vesicles (Barratt and Laggner, 1974; Sanson et al., 1976; Egret-Charlier et al., 1978; Ptak et al., 1980), the origin of the spectral heterogeneity has not been unambiguously assigned to changes in the ionization of the carboxyl group on the fatty acid derivative. Therefore, to clarify the source of the observed spectral heterogeneity, we have reinvestigated the ionization state of fatty acid linked spectroscopic probes. We have used vesicles made from DMPC as a model system since this phospholipid structure has been extensively characterized (Pearson and Pascher, 1979; Lange et al., 1985; Moser et al., 1989; reviewed by Hauser et al., 1981; Seelig et al., 1987), and it forms a relatively homogeneous population of neutral phospholipids with essentially no titratable groups (i.e., $pK_{PO4} < 1$) (Cevc and Marsh, 1987).

The spin-label EPR technique has proven to be very sensitive to small changes in the mobility of phospholipid fatty acyl chains due to its appropriate time-scale ($T_2 \simeq 10^{-8}$ s) and orientational resolution (as little as 8°; Thomas, 1985), and therefore provides the optimal sensitivity to any environmental heterogeneity with respect to the positioning of the nitroxide on the fatty acyl chain relative to the membrane normal. ^{15}N-5-stearic acid spin labels (5-SASL) were used to gain the resolution necessary to assess the presence of multicomponent spectra, since the larger hyperfine coupling constant and the reduced nuclear manifolds ($I = 1/2$) for ^{15}N result in much narrower, better resolved lineshapes (Keith et al., 1974). Due to the large polarity gradient and motional constraints near the membrane surface (Griffith et al., 1974; Scherer, 1989), a nitroxide was chosen that is near the membrane surface (i.e., at the 5 position), thereby maximizing spectral differences that arise as a result of vertical displacements relative to the membrane surface. We have investigated the dynamics of stearic acid spin labels on both the time-scale of T_2 (ns) and T_1 (μs), utilizing conventional and saturation recovery EPR to better define the underlying cause of the observed spectral changes. However, the relationship between the spectral populations observed in the EPR spectrum to a physical model describing the probe's mobility is ambiguous due to the spin label's sensitivity to many other environmental factors including polarity changes, dipolar interactions, and H-bonding. Therefore, we have used time-resolved optical measurements of the lifetime and anisotropy of fluorescent lipid probes to distinguish between changes in the relaxation properties of the fluorophore and motional effects. By comparing the lifetime and anisotropy of a fluorescent fatty acid (i.e., 2-AS) and a phospholipid analogue (i.e., DPH-PC) we have been able to distinguish between effects relating to the degree of ionization of the stearic-acid label from changes in membrane structure, allowing us to unambiguously interpret the effect of changes in temperature and ionic strength on the conformation of model membranes composed of dimyristoyl phosphatidylcholine.

MATERIALS AND METHODS

Materials

PIPES (Piperazine-*N*,*N*′-bis[2-ethanesulfonic acid]), CHES (2-[*N*-cyclohexylamino]ethanesulfonic acid), EPPS (*N*-[2-hydroxyethyl]-piperazine-*N*′-[3-propane)sulfonic acid]), sodium acetate, sodium bicarbonate, and DMPC (dimyristoylphosphatidylcholine) were obtained from Sigma Chemical Co. (St. Louis, MO). 2-AS (2-(9-anthroyloxy) stearic acid) and DPH-PC (2-(3-(diphenylhexatrienyl)propanoyl)-3-palmitoyl-L-α-phosphatidylcholine) were obtained from Molecular Probes Inc. (Junction City, OR). The ^{15}N-5-stearic acid spin label (5-SASL or 5-doxyl stearic acid) was synthesized by Dr. Joy Joseph (after the procedure of Hubbell and McConnell, 1971; Joseph and Lai, 1988), and was generously supplied for our use.

Probe incorporation and lipid vesicle formation

The spin-labeled or anthroyloxy derivatives of stearic acid or the DPH-PC phospholipid analogue (Fig. 1) were diluted from a stock solution in chloroform into ethanol before addition to organic dispersions of DMPC at a ratio of less than one label to 200 phospholipids. The lipids were subsequently dried under a stream of nitrogen and placed under vacuum overnight to remove any traces of remaining solvent. The lipids were then dispersed in the experimental buffer and either (*a*) vortexed (forming multilammelar vesicles for EPR experiments) or (*b*) sonicated and subsequently centrifuged at 40,000 × *g* for 30 min to remove nonsolubilized material (forming unilammelar vesicles for fluorescence experiments; Lakowicz et al., 1979; Bocian and Chan, 1978). For EPR experiments the lipid concentration was made sufficiently high (>100 mM) so that the conventional EPR spectrum contained a negligible contribution from unbound spin labels, while the lipid concentration was ~1 mM for the fluorescence studies. The pH of these zwitterionic membrane samples was maintained by 20 mM buffer at 1 mol percent stearic acid probe, as judged by electrode measurements.

EPR measurements

(a) Conventional EPR

EPR spectra were obtained with a Varian E-109 spectrometer (Varian Associates, Palo Alto, CA) and spectra were digitized and analyzed with a IBM-PC computer interfaced to the spectrometer. The rotational motion of stearic-acid spin labels (SASL) was detected using 100-kHz field modulation with a peak-to-peak amplitude (H_m) of 0.1 Gauss. A nonsaturating microwave field intensity (H1 ≃ 0.03 Gauss) was used, thereby ensuring that the spectral shape is not distorted by saturation effects and is an accurate representation of the rotational dynamics on the nanosecond time-scale.

In analogy to ^{14}N spin label EPR spectra, $T'_\parallel$ and $T'_\perp$ are defined as the measured outer and inner splitting (in Gauss) resolved in the EPR spectrum of ^{15}N-SASL in DMPC membranes (see Fig. 2), where $T_\parallel$ and $T_\perp$ are the principal values of the hyperfine tensor for an axially

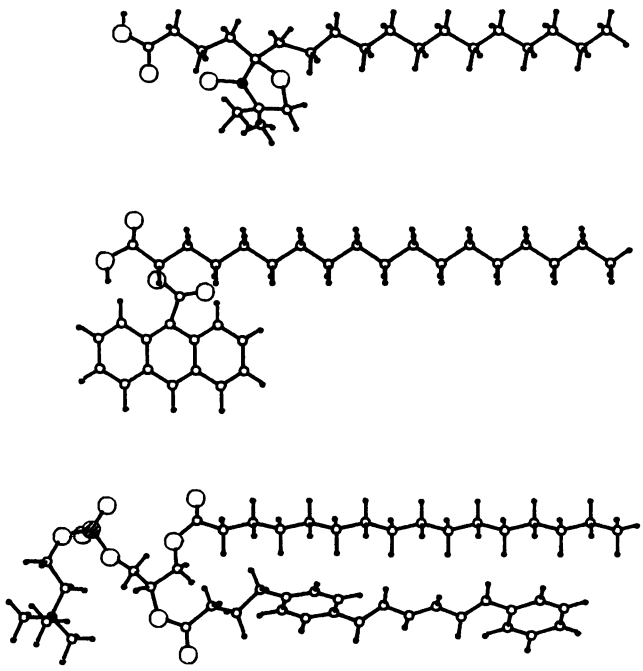

FIGURE 1 Ball and stick representation of spin-labeled and fluorescent lipid analogues used in this study include 5-SASL (*top*) and 2-AS (*middle*) which are *N*-oxyl-4′,4′-dimethyloxazolidine and 9-anthroyloxy derivatives of stearic acid, respectively. DPH-PC (*bottom*) is a 3-(diphenylhexatrienyl) propanoyl analogue of dipalmitoyl phosphatidycholine, in which the polyene chromophore substitutes for palmitic acid in the sn2 chain. The elements depicted are: H (*small open circles*), C (*medium open circles*), O (*large open circles*), N (*medium closed circles*), and P (*large stippled circles*).

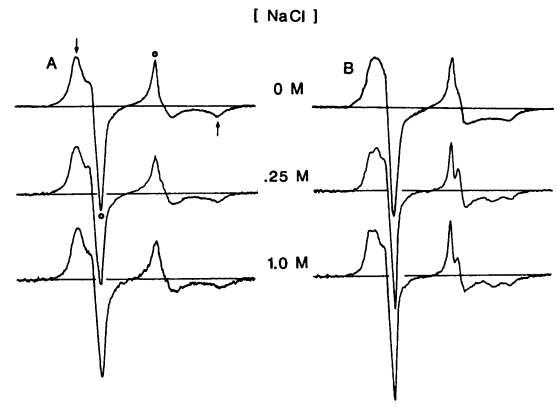

FIGURE 2 Ionic strength dependence of EPR spectra for ^{15}N-5-SASL at 30°C (*A*) and 50°C (*B*). Spectra are recorded under nonsaturating field intensities ($H_1 < 0.05$ Gauss) in 20 mM PIPES and the indicated salt concentration. The pH was readjusted to maintain pH 7.0 as a function of salt concentration and temperature. All spectra were recorded in-phase using 100 kHz field modulation with a peak-to-peak amplitude of 0.1 Gauss and a 60 Gauss scan range. The distance between the outer extrema (indicated by arrows) is $T'_\parallel$, whereas the distance between the inner extrema (indicated by open circles) is $T'_\perp$. The low-field linewidth ($\Delta W_{1/2}$) is defined as the half width at half height.

symmetric system (e.g., a lipid bilayer). T'_o is the apparent isotropic hyperfine splitting constant in the absence of anisotropic effects, and is diagnostic of the polarity of the label (Seelig, 1970; Marsh, 1981), and is defined as:

$$T'_o = 1/2(T'_\parallel + T'_\perp). \quad (1)$$

(*b*) Saturation-recovery EPR (SR-EPR)

The SR-EPR spectrometer equipped with a loop-gap resonator has been described previously (Fajer et al., 1986; Yin et al., 1988). A field-effect transistor (FET) microwave amplifier with a time-response of 0.1 μs was used. Typically 20,000 decays per second were acquired with 512 data points on each decay. The total accumulation time was typically 30 min per sample. Aperture intervals were 60 ns. The decay was observed at a field position corresponding to the maximal spectral intensity, using a modulation amplitude of 1.0 Gauss, and a modulation frequency of 25 Hz.

All saturation recovery studies were done subsequent to the removal of molecular oxygen, since O_2 will artificially shorten the spin-lattice relaxation time (T_1). Oxygen was removed from reference and experimental samples using gas-permeable sample cells made from methylpentene polymers (TPX) purged with N_2 for 30 min at 25°C (Popp and Hyde, 1981; Yin et al., 1988). Temperature was controlled to within 0.5°C with a Varian V4540 variable temperature controller (Varian Associates, Inc., Palo Alto, CA). During data acquisition the temperature was monitored with a digital thermometer (model 2100A; John Fluke Manufacturing Co., Seattle, WA), in which the probe was positioned above the sample in the center of the cavity. The resulting saturation recovery data was analyzed utilizing a multiexponential model using a Gauss-Newton minimization procedure as described previously (Yin et al., 1987).

Fluorescence measurements

Steady-state fluorescence measurements were performed on an SLM 8000 photon counting spectrofluorometer using 366 nm excitation with emission observed through a Corning 3-73 cutoff filter. The steady-state anisotropy, *r*, was calculated from the ratio of the fluorescence intensities with the polarizers in the vertical (v) or horizontal (h) position:

$$r = (I_{vv} - GI_{vh})/(I_{vv} + 2GI_{vh}), \quad (2)$$

where $G = I_{hv}/I_{hh}$, and corrects for the differing sensitivities of the detection system for vertically and horizontally polarized light (Lakowicz, 1983).

Frequency-domain measurements were performed on an instrument described previously (Lakowicz et al., 1986*a*,*b*). The modulated excitation was provided by the harmonic content of a laser pulse train with a repetition rate of 3.79 MHz and a pulse width of about 8 ps, from a synchronously pumped and cavity-dumped pyridine-2 dye laser. The dye laser was pumped with a mode-locked argon ion laser (Coherent, Innova 15). The dye laser output was frequency doubled to 366 nm with an angle-tuned KDP crystal. The emitted light was observed with a microchannel photomultiplier, and the cross-correlation detection was performed outside the PMT. The emission was observed through a Corning 3-73 broad band emission filter. For intensity decay measurements, magic angle polarizer orientations were used.

(a) Decays of fluorescence intensity

The intensity decay was analyzed assuming either a multiexponential decay or a distribution of decay times (Alcala et al., 1987; James et al., 1987; Lakowicz et al., 1987*a*,*b*; 1988*a*). For the case of a multiexponential decay, the impulse response $I(t)$ is given by:

$$I(t) = \Sigma_i \alpha_i \exp(-t/\tau_i), \quad (3)$$

where α_i is the pre-exponential factor and τ_i is the decay time. Alternatively, we assumed that the individual components were distributed as a unimodal distribution of lifetimes involving either a Lorentzian or Gaussian lineshape. The parameters are determined by the method of nonlinear least squares (Bevington, 1969; Lakowicz et al., 1984; Gratton et al., 1984).

(b) Decays of fluorescence anisotropy

Time-resolved anisotropies, $r(t)$, were determined from the phase angle difference (Δ_ω) between the perpendicular ($\phi_\perp$) and parallel ($\phi_\parallel$) components of the modulated emission ($\Delta_\omega = \phi_\perp - \phi_\parallel$) and from the ratio of the amplitudes (Λ_ω) of the parallel ($m_\parallel$) and perpendicular ($m_\perp$) components of the modulated emission ($\Lambda_\omega = m_\parallel/m_\perp$). These values are compared with those expected for an assumed anisotropy decay law. In general $r(t)$ can be described as a multiexponential decay:

$$r(t) = r_o \Sigma_i g_i \exp(-t/\phi_i), \quad (4)$$

where r_o is the limiting anisotropy in the absence of rotational diffusion, ϕ_i are the rotational correlation times, and g_i are the fractions of the total anisotropy loss associated with each correlation time. The *hindered rotator model* is a particular case of this general expression, one of the ϕ_i being equal to infinity and the corresponding $r_o g_i = r_\infty$, i.e.,

$$r(t) = (r_o - r_\infty)\Sigma_i g_i \exp(-t/\phi_i) + r_\infty. \quad (5)$$

The frequency-dependent values of the phase angle difference (Δ_ω) and the ratio of the modulation amplitudes (Λ_ω) are given by Lakowicz et al. (1985). For all least-squares fits we used an independently measured value of r_o, determined at −60°C in propylene glycol (see legends for Tables). In general the errors in Δ_ω were estimated to be 0.2 deg and in Λ_ω to be 0.02.

RESULTS

Ionic strength-dependent changes in the spin label EPR spectra

In agreement with previous reports we find that at 50°C and high ionic strengths multicomponent spectra are observed for 5-SASL in DMPC membranes at pH 7.0 (Fig. 2*B*) (Barratt and Laggner, 1974; Sanson et al., 1976; Egret-Charlier et al., 1978; Ptak et al., 1980). As a result of the narrower line widths characteristic of the ^{15}N-nitroxide label used in this study we have been able to explore the effects of more physiological temperatures and ionic strengths on the spectral heterogeneity. Under these conditions (i.e., 30°C and/or low ionic strengths) we observe essentially a single-component spectrum (Fig. 2). At 50°C there is an ionic strength-dependent appearance of a spectral component with a narrower maximal splitting, especially apparent in the high field peak. In contrast to these results, at 30°C the spectra remain characteristic of a single motional population (Fig. 2*A*). The ionic strength dependence is not related to the particular ionic species since either KCl or Na_2HPO_4 produce a similar ionic strength dependence (data not shown), indicating that specific ionic associations are not occurring with the phosphatidylcholine headgroups. These ionic strength-dependent changes are therefore probably related to either (*a*) changes in the ionization state of the α-carbonyl group on the stearic-acid spin label or (*b*) relaxation and/or motional effects that are modulated by the phospholipid structure. To distinguish between these possibilities it is first necessary to establish the pK_a of the stearic-acid spin label under these experimental conditions, where the pk_a measured in this study represents the bulk pH at which half of the protons on the α-carbonyl of the stearic acid are dissociated.

Determination of stearic-acid spin label's pK_a

The spectra of 5-SASL in DMPC vesicles undergo a pH-dependent change in which the maximal splitting ($T'_\parallel$) or the apparent hyperfine coupling constant (T'_o) increases as the α-carbonyl group is deprotonated (Fig. 3 and Table 1). Quantitation of the relationship between $T'_\parallel$ (or T'_o) and the pH indicates that the pK_a of 5-SASL

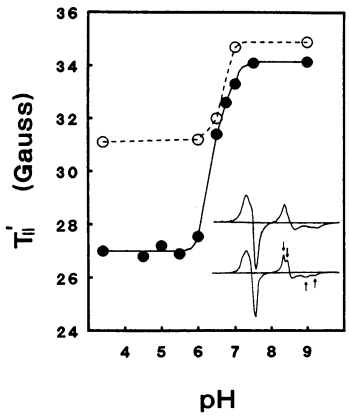

FIGURE 3 pH-dependence of $T'_\parallel$ for ^{15}N-5-SASL at 30°C (*open circles*) and 50°C (*closed circles*). Spectral conditions were as in the legend of Fig. 2. The buffer consisted of either 20 mM sodium acetate (pH 3.4., 4.5, 5.0, or 5.5), 20 mM sodium bicarbonate (pH 5.5), 20 mM PIPES (pH 6.0, 6.5, 7.0, or 7.5), or 20 mM CHES (pH 9.0). The inset illustrates the spectra obtained at pH 6.5 at either 30°C (*top spectrum*) or 50°C (*bottom spectrum*). Arrows illustrate the heterogeneity observed in the high-field region of the spectrum at 50°C. In all cases the pH was confirmed using an ion electrode prior to the experimental measurement.

TABLE 1 **pH and ionic strength-dependent changes in the spectral properties of ^{15}N-5-Stearic acid spin label at 30°C in DMPC vesicles**

pH	[NaCl]	Conventional EPR (*Gauss*)[a]				Saturation recovery	
		$T_{\parallel}'$	$T_{\perp}$	T_o	$\Delta W_{1/2}$	T_1	χ^2_R
						us[b]	
3.4	0.02 M	31.1	15.1	23.1	1.8	5.6	1.22
6.0	0.02 M	31.3	14.7	23.0	2.0	—	—
6.5	0.02 M	32.0	14.0	23.0	1.8	—	—
7.0	0.02 M	34.8	13.3	24.1	1.5	6.0	0.88
9.0	0.02 M	34.9	13.3	24.1	1.2	6.5	1.66
7.0	0.50 M	34.5	13.6	24.1	1.9	5.7	1.33
7.0	1.0 M	34.5	13.4	24.0	1.9	5.8	1.36

The conventional and saturation recovery measurements are described in Methods. Relative errors in the measurements are: [a]±0.2 Gauss; [b]±0.1 μs. Buffer conditions included 20 mM Sodium Acetate (pH 3.4); 20 mM Sodium Bicarbonate (pH 6.0); 20 mM PIPES (pH 6.0, 6.5, and 7.0); 20 mM CHES (pH 9.0). T_o', the apparent isotropic hyperfine splitting constant, is given by: $T_o' = 1/2(T_{\parallel}' + T_{\perp}')$, where $T_{\parallel}'$ and $T_{\perp}'$ are defined in the legend to Fig. 2. $\Delta W_{1/2}$ is defined as the low-field linewidth at half-height.

is 6.3 and 6.6 at 50° and 30°C, respectively, in close agreement with previous studies utilizing SASL in biological membranes (Esmann and Marsh, 1985). Likewise, previous measurements indicate the pK_a of stearic acids to be weakly dependent on the temperature, increasing ~0.3 pH units upon lowering the temperature 20°C (Egret-Charlier et al., 1978; Ptak et al., 1980). A comparison of the maximal splitting ($T_{\parallel}'$) observed at 30° and 50°C indicates that there is a much larger change in $T_{\parallel}'$ at 50°C relative to that observed at 30°C, indicating either a larger motional and/or polarity change sensed by the nitroxide group upon ionization of the stearic acid's α-carbonyl.

Multiple environments are observed for 5-SASL near the pK_a at 50°C (Fig. 3, *inset*). In contrast, the spectra recorded at 30°C remain characteristic of a single population of spin labels over the entire pH range studied, even near the pK_a. This suggests that at 30°C the nitroxide samples a single environment relative to the membrane normal, irrespective of the degree of ionization on the α-carbonyl group. The effect of the ionization state of the α-carbonyl on the relaxation properties and/or dynamics of the nitroxide is therefore different at 30° and 50°C, suggesting that the surrounding phospholipids have undergone a temperature-dependent change in their average conformation.

Relaxation properties of stearic acid spin labels

To better distinguish between spectral effects related to ionization of the stearic acid label from environmental effects that alter the nitroxide's relaxation properties we have used saturation-recovery EPR (SR-EPR) to directly measure the relaxation properties of the stearic acid spin label as a function of the pH. Typical magnetization recoveries for the ^{15}N-5-SASL probe are shown in Fig. 4 and the relaxation time obtained from the data is shown in Table 1. The illustrated trace was recorded subsequent to a long saturating pulse (i.e., 5 μs), thereby ensuring that the entire spin system is saturated, and that the measured recovery is related only to the relaxation properties of the system and is not complicated by the presence of spectral diffusion (Fajer et al., 1986). Identical results are obtained for short pulses (i.e., 0.4 μs), indicating that spectral diffusion is much faster than T_1, and that the entire spin system is motionally averaged. In all cases a single-exponential

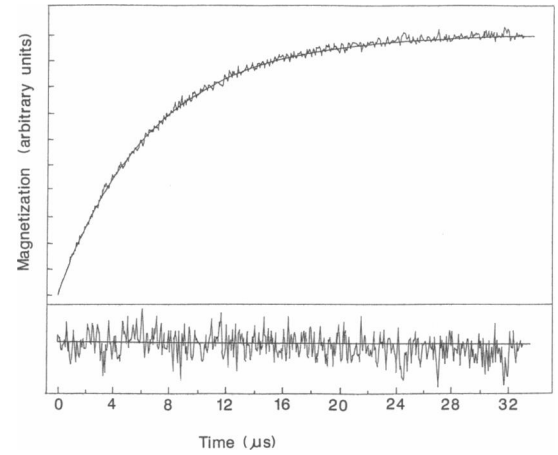

FIGURE 4 Saturation-recovery signal of ^{15}N-5-SASL (1 mol %) in DMPC liposomes at 30°C, pH 7.0 (20 mM PIPES). The magnetization recovery signal was obtained in ~30 min at 20,000 accumulations per second, 512 data points per accumulation. This trace was obtained with a 5.0 μs pulse using 12 dB pump and 30 dB probe. The data were fit to a single exponential model where the goodness of fit was judged by the residual plot, which is expanded five-fold for greater clarity.

model was adequate to fit the data, as judged by the residuals, in which the actual data is apparently randomly displaced about the single exponential fit. However, the possibility that the observed single-exponential decay is a result of a rapid physical exchange (faster than T_1) between spin labels in two different environments in the membrane cannot be unambiguously ruled out at present.

We observe that upon increasing the pH from 3.4 to 7.0, there is a small, but reproducible increase in the relaxation time, T_1 (Table 1). T_1 continues to change as the pH is increased from pH 7.0 to 9.0 well beyond the point where the fatty acids are completely ionized. This indicates that the pH-dependent changes in the relaxation properties of the spin label are not uniquely correlated with the ionization of the α-carbonyl group on the fatty acid, and suggests that the pH-dependent changes in the spectral linewidth are responding to the relaxation properties of the label. Upon increasing the ionic strength (pH 7.0) T_1 further decreases, while the linewidth ($\Delta W_{1/2}$) increases (Table 1), consistent with the expected relation between these parameters. We currently do not have an explanation for this phenomena, but pH and/or ionic strength-dependent changes in the hydration properties and/or dipolar interactions between the nitroxide and either the phospholipid or aqueous environment within the bilayer may be involved.

Ambiguity within spin-label EPR measurement

Although the orientational resolution inherent in spin-label EPR measurements result in an optimal sensitivity to membrane heterogeneity, the spectra are modulated by both the degree of ionization of the α-carbonyl on the stearic acid spin label and by changes in the spin label's relaxation properties (see above). Therefore, to quantitatively understand these pH and/or ionic strength-dependent changes in terms of a physical model, we have made use of time-resolved measurements of the fluorescence intensity decays and anisotropy of both 2-AS and DPH-PC incorporated in DMPC vesicles. 2-AS, a stearic-acid derivative, is analogous to 5-SASL in that the spectroscopic probe is located on the fatty acyl chain near the α-carbonyl. DPH-PC is a phospholipid analogue and has no titratable groups in the pH range of interest (i.e., 3.4–9.0). Therefore, pH and/or ionic strength dependent changes in the lifetime or mobility of DPH-PC can be uniquely understood in terms of the bilayer structure.

Intensity decay of DPH-PC in vesicles of DMPC

We have examined the lifetime of DPH-PC in DMPC using frequency-domain fluorescence spectroscopy, since the lifetime of fluorescent probes is modulated by the environment of the probe and will therefore sense changes in membrane structure. An example is shown in Fig. 5, at 30°C. As the frequency is increased, one observes increased demodulation, or an increasing phase angle relative to the incident light, that can be used to determine the lifetimes related to the fluorophore (e.g., α_i, τ_i; Table 2). The data could not be fit with a single-exponential model, but requires a double-exponential model, resulting in a 2–3 fold decrease in χ^2_R. With 15 degrees of freedom, a two-fold decrease in χ^2_R indicates with 98% confidence that the two-exponential decay model is required (Bevington, 1969). While the data are consistent with a multiexponential model, this does not demonstrate that the decay is uniquely described by two decay times. We therefore also analyzed the data using models in which the intensity decay is fit to either a Lorentzian or Gaussian distribution of decay times

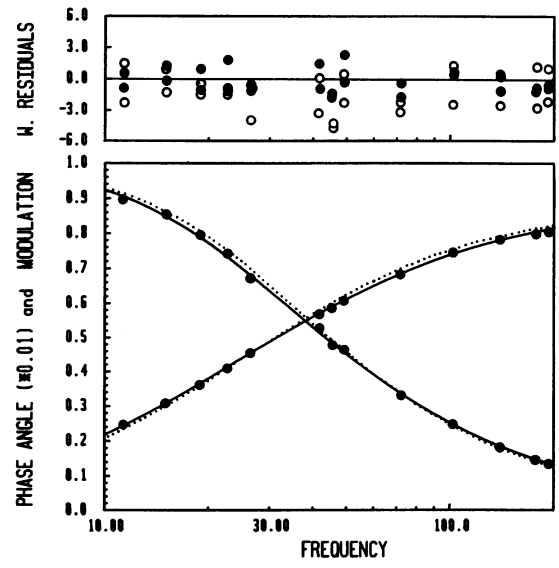

FIGURE 5 Lifetime-resolved emission of DPH-PC in DMPC vesicles at 30°C. As the frequency (in MHz) is increased the phase angle (in degrees) of the emission increases while the modulation decreases (see Methods). The closed circles show the data and the curves the best single (*dotted line*) and double (*solid line*) exponential fits to the data. The upper panel shows the weighted residuals between the best single (*open circles*) and double (*closed circles*) exponential fits for both the phase and modulation data. The weighted residuals are defined as the absolute difference between the experimental data and the fit to the exponential model, normalized by the standard deviation of the measurement. Buffer conditions included 20 mM PIPES (pH 7.0).

TABLE 2 **Multiexponential analysis of emission from DPH-PC in DMPC**

Sample	$\langle\tau\rangle$	τ_1	α_1	τ_2	α_2	χ^2_R
	ns	*ns*		*ns*		
30°C						
pH 3.4	6.39	3.92	0.34	7.09	0.66	1.18 (4.2)[b]
pH 7.0	6.42	3.12	0.24	6.88	0.76	1.47 (5.3)
pH 9.0	6.40	2.68	0.16	6.69	0.84	2.39 (4.1)
pH 7.0/pH 3.4[c]						1.48
pH 9.0/pH 3.4						2.47
50°C						
pH 3.4	5.59	1.86	0.14	5.78	0.86	0.96 (4.2)
pH 7.0	5.62	1.21	0.12	5.74	0.88	1.57 (4.4)
pH 9.0	5.62	2.24	0.18	5.91	0.82	1.72 (4.5)
pH 7.0/pH 3.4						1.67
pH 9.0/pH 3.4						1.52
50°C; 1.0 M KCl:						
pH 3.4	5.44	2.06	0.16	5.68	0.84	1.27 (5.1)
pH 7.0	5.50	2.54	0.18	5.79	0.82	1.86 (5.7)
pH 9.0	5.48	3.71	0.45	6.34	0.55	0.92 (3.7)
pH 3.4; no salt/pH 3.4: 1.0 M KCl						5.1
pH 7.0; no salt/pH 7.0: 1.0 M KCl						4.6
pH 9.0; no salt/pH 9.0: 1.0 M KCl						5.1

[a]Calculated from $\langle\tau\rangle = [\Sigma_i\alpha_i\tau_i^2/\Sigma_i\alpha_i\tau_i]$; the standard deviation of $\langle\tau\rangle$ is typically ±0.1 ns. [b]The bracketed number corresponds to the χ^2_R for the single exponential fit to the data. [c]The data from the first listed sample (before slash) were force fit with the parameters from the fit for the second listed sample (after slash).

(Alcala et al., 1987; James et al., 1987; Lakowicz et al., 1987). The data could be satisfactorily fit with a unimodal distribution assuming either the Lorentzian or Gaussian lineshape, resulting in values of χ^2_R that are essentially equivalent to those found with the two-exponential decay-time model (Table 2 and Fig. 6). It should be noted that the distribution models contain only two floating parameters, and are therefore intermediate in complexity between one and two-exponential decay models that have one and three floating parameters, respectively. Given that the χ^2_R for the distribution analysis is more similar to the two-exponential decay, this result provides some support that there is in fact a distribution of decay times for DPH-PC in DMPC bilayers. However, while the experimental data cannot be used to unambiguously select any of the models as correct, we do believe the lifetime distribution plots provide a useful visualization of the intensity decay.

We have therefore investigated the pH and ionic strength dependence of the intensity decay of DPH-PC in vesicles of DMPC using all three models, to ask whether there are any changes in the bilayer structure that might explain the spectral changes observed using the 5-SASL label. The parameters describing the intensity decay of DPH-PC (assuming a multiexponential model) are summarized in Table 2. The spectral parameters obtained at the different pH values are quite similar and there are no pH-dependent changes in the

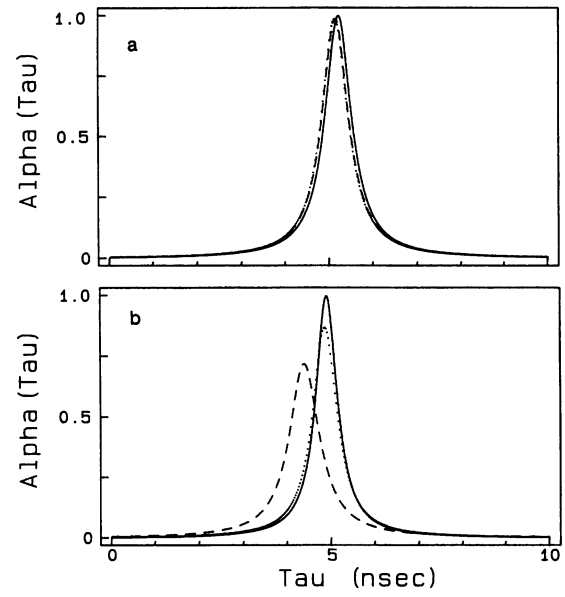

FIGURE 6 Relationships between recovered lifetime distributions and pH for DPH-PC (*a*) and 2-AS (*b*). The intensity decays in DMPC vesicles were fit to a Lorentzian distribution (see Methods), and the respective areas associated with each distribution was arbitrarily normalized relative to the maximal peak height observed at pH 7.0. Buffer conditions included either 20 mM Sodium Acetate (pH 3.4; *dashed line*); 20 mM PIPES (pH 7.0; *solid line*), and 20 mM CHES (pH 9.0; *dotted line*). The weighted residuals at pH 3.4, 7.0, and 9.0 yielded χ^2_R values of 1.3, 2.3, and 2.0 for DPH-PC and 4.0, 3.6, and 3.3 for 2-AS, respectively. Sample temperature = 50°C.

mean decay time (i.e., $\langle\tau\rangle$), or alternatively in the lifetime distribution parameters (i.e., the mean lifetime or width of the distribution; Fig. 6 *A*). We do, however, observe a small but significant decrease in the mean decay time at 50°C when the ionic strength is increased, irrespective of the pH of the measurement. At the lower ionic strength the mean decay time (i.e., $\langle\tau\rangle$) obtained from the multiexponential model at the three measured pH's is 5.61 ns, as compared with 5.47 ns at the higher ionic strength; likewise there is a similar difference between the lifetime-distribution parameters at 50°C (data not shown), consistent with a more polar environment around the label at the higher ionic strength.

The decrease in the mean decay time is experimentally reproducible and statistically significant as evidenced by force fitting the data for each sample with the parameters to the alternative sample (Table 2). For comparison of the high ionic strength conditions with that at low ionic strength, the value of χ^2_R increased four-fold (using either the multiexponential or lifetime distribution models), indicating that with 22 degrees of freedom there is less than a one percent probability that the data represent the same intensity decay.

Anisotropy decays of DPH-PC

The anisotropy of the probe DPH has been suggested to be an indicator of the microviscosity of biological membranes (Shinitzky and Barenholz, 1974), and the residual anisotropy (i.e., r_∞) has been interpreted in terms of the order parameter of the bilayer (Kinosita et al., 1977; Heyn, 1979; Jahnig, 1979; Lipari and Szabo, 1980). The DPH-PC probe has been subsequently introduced to avoid potential problems associated with the orientational specificity of DPH in the bilayer, since DPH has been shown to partition into multiple environments (Prendergast et al., 1981). While a number of charged analogues of DPH have been introduced to position the probe at the interface (e.g., TMA-DPH), DPH-PC has the advantage that it is a phospholipid analogue and therefore has no titratable groups over the measured pH range, indicating that any changes in it's relaxation or dynamic properties can be unambiguously interpreted in terms of the bilayer's structure.

The differential polarized phase angles and modulated anisotropy of DPH-PC in DMPC was measured as a function of pH and ionic strength. An example is shown in Fig. 7. Single or double correlation time models were not adequate to describe the decay (Table 3). The best results, as indicated by the approximately twenty-fold reduction in the value of χ^2_R in comparison to the two-component model, required three correlation times (Table 3); one of the correlation times is typically

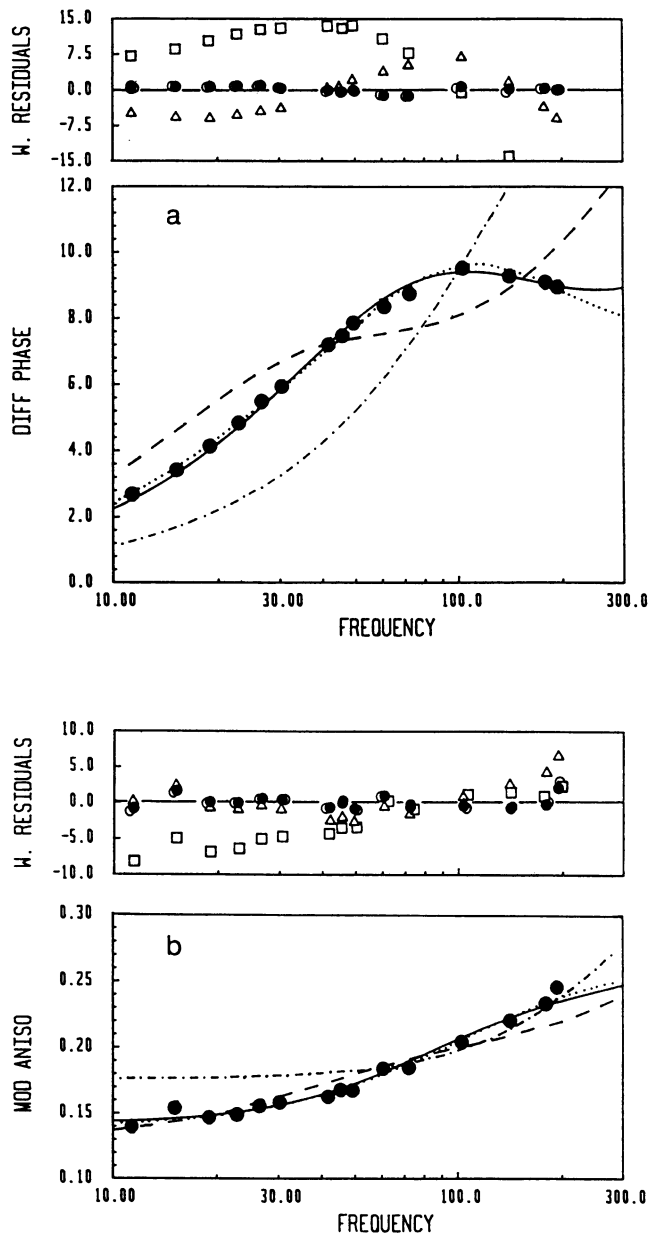

FIGURE 7 Differentially polarized phase angles (degrees) (*a*) and modulated anisotropy ratios (*b*) as a function of the frequency (in MHz) of the amplitude modulated light for DPH-PC in vesicles made from DMPC (30°C, pH 7.0). The closed circles represent the data and the curves represent the best fits to the data using models (see Methods) involving (*a*) a single correlation time with a nonzero r_∞ (*dot-dashed line*), (*b*) two correlation times (*dashed line*), (*c*) two correlation times with a nonzero r_∞ (*solid line*), and (*d*) three correlation times (*dotted line*). The weighted residuals are shown for the various models above the frequency dependence of both the differential phase (in degrees) and the modulation anisotropy, and are weighted relative to the standard deviation of the measurement, i.e., $\sigma p = 0.2°$ and $\sigma m = 0.02$. The symbols relating to the respective models are: model (*a*) open squares; model (*b*) open triangles; model (*c*) closed circles; and model (*d*) open circles, respectively.

TABLE 3 **Anisotropy decay parameters for diphenylhexatriene-phosphatidylcholine in lipid vesicles made from dimyristoylphosphatidylcholine at 30°C, pH 7.0[a]**

Model	θ_1	θ_2	θ_3	g_1	g_2	g_3	r_∞	χ^2_R
	ns	*ns*	*ns*					
1 θ	0.24			1.00				607
θ, r_∞	0.55			0.60			0.16	116
2 θ	0.26	11.0		0.50	0.50			15.1
2 θ, r_∞	0.12	2.7		0.38	0.39		0.09	0.88
3 θ	0.08	2.0	54	0.11	0.37	0.28[b]		0.64

[a] r_0 was held constant at 0.393, the anisotropy of DPH-PC at −60°C in propylene glycol, 366 nm excitation. The estimated errors were $\Delta_\infty = 0.2$ degrees and $\Lambda_\infty = 0.02$. The measured lifetimes are listed in Table 2. [b] In this case $r_\infty \cong g_3\theta_3 = 0.11$.

quite long (i.e., greater than 50 ns), resulting in the inability to distinguish between the three correlation time model (*dotted line* Fig. 7) and a two-correlation time model involving motional restriction (hindrance; *solid line,* Fig. 7). We emphasize that the three correlation time model is equivalent to the two correlation time motionally restricted model, and the long correlation time (i.e., ϕ_3) may be regarded as a hindered motion with an amplitude given by $r_0 x g_3$ (Table 3). However, in all fitting procedures that employ multiple floating parameters one must ultimately rely on other information for selecting between models that predict similar data. Because biological membranes are highly ordered two-dimensional liquid crystals, there is reason to expect that the motion of a conjugated and hence relatively rigid polyene chain will undergo a considerable degree of orientational constraint (Bocian and Chan, 1978). We therefore arbitrarily report the parameters resulting from the two correlation time model involving motional restriction for comparative purposes between different experimental conditions. We do however note the close agreement between the resolved parameters in Table 5 and earlier measurements that have identified multiple correlation times on both the subnanosecond and nanosecond time-scales, that are predicted to correlate with both the trans-gauche isomerizations and overall rotational mobility of the phospholipid acyl chains, as well as a residual anisotropy correlating with the motional restriction associated with the order parameter of the membrane (Seelig and Seelig, 1980; Deese and Dratz, 1986; Moser et al., 1989). Furthermore, the degree of hindrance observed in the present investigation compares favorably with previous studies utilizing DPH in single component membranes containing DMPC (Lakowicz et al., 1985).

Analysis of ionic strength and pH dependence of DPH-PC

Having established a suitable model to describe the probe's mobility, we investigated the pH and ionic strength dependence of the differential phase and modulated anisotropy of DPH-PC in vesicles of DMPC to further clarify the spectral changes observed using the stearic-acid spin labels. The frequency-domain data are summarized in Table 4. The spectral parameters are quite similar and there are no statistically significant *pH-dependent* changes in the correlation times or amplitude factors as judged by force fits of the data for each sample with the parameters to the alternative samples; representative examples of the values of χ^2_R obtained when the parameters associated with the conditions involving pH 3.4 were fit to the data taken at pH 7.0 and 9.0 are shown in Table 4. We do, however, observe a small, but significant increase in the residual anisotropy (i.e., r_∞ from Eq. 15) at 50°C when the ionic strength is increased. At the lower ionic strength the average residual anisotropy measured at three different pH's is 0.042 ± 0.003, as compared with 0.056 ± 0.005 at the higher ionic strength. The correlation times relating to the rotational mobility of the fatty acyl chains are not significantly altered by the ionic strength. The increase in the residual anisotropy is experimentally reproducible and statistically significant as evidenced by force fitting the data with the parameters corresponding to the alternative sample.

Thus the results of both lifetime and anisotropy measurements of DPH-PC indicate that there are no pH-induced alterations in the bilayer structure, but there is an effect of ionic strength which acts to decrease the average lifetime and increase the residual anisotropy at 50°C.

Intensity decay of 2-AS in vesicles of DMPC

Anthroyloxy stearate probes are in many ways analogous to stearic acid spin labels in that the probes have been well characterized and position themselves at well defined positions relative to the membrane normal, the α-carbonyl aligning itself with the polar headgroup of the phospholipids (Thulburn and Sawyer, 1978). There-

TABLE 4 **Anisotropy decay parameters for diphenylhexatriene-phosphatidylcholine in dimyristoylphosphatidylcholine as a function of pH, temperature, and ionic strength**

Sample[a]	$\langle\tau\rangle$	θ_1	θ_2	g_1	g_2	r_∞	χ^2_R
	ns	*ns*	*ns*				
30°C							
pH 3.4	6.39	0.12	2.9	0.40	0.39	0.085	0.83 (13.6)[b]
pH 7.0	6.42	0.12	2.7	0.38	0.39	0.092	0.88 (15.1)
pH 9.0	6.40	0.15	2.9	0.40	0.37	0.091	1.31 (4.9)
pH 7.0/pH 3.4[c]							1.55
pH 9.0/pH 3.4							1.35
50°C							
pH 3.4	5.59	0.05	1.7	0.40	0.48	0.045	2.7 (13.9)
pH 7.0	5.62	0.14	2.0	0.48	0.42	0.040	1.4 (7.8)
pH 9.0	5.62	0.09	1.8	0.45	0.45	0.041	1.0 (8.5)
pH 7.0/pH 3.4							2.1
pH 9.0/pH 3.4							1.5
50°C; 1.0 M KCl:							
pH 3.4	5.44	0.14	2.1	0.46	0.41	0.053	1.7 (8.9)
pH 7.0	5.50	0.17	2.1	0.42	0.42	0.061	0.77 (9.8)
pH 9.0	5.48	0.13	2.1	0.42	0.44	0.053	0.57 (9.0)
pH 3.4; no salt/pH 3.4: 1.0 M KCl M KCl							4.2
pH 7.0; no salt/pH 7.0: 1.0 M KCl M KCl							8.6
pH 9.0; no salt/pH 9.0: 1.0 M KCl M KCl							9.6

[a]The standard errors are typically ±31% for θ_1; ±12% for θ_2; ±8% for g_1; ±7% for g_2; ±8% for r_∞. [b]The bracketed number corresponds to the X^2_R for the 2 correlation time model. [c]The data from the first listed sample (before slash) were force fit with the parameters from the fit for the second listed sample (after slash). Standard errors for the phase and modulation measurements were 0.2 degrees and 0.02, respectively. r_o was determined to be 0.393 from steady state measurements of fluorescence anisotropy taken in propylene glycol at −60°C (see Eq. 2 in Methods).

fore, having determined that there are no pH-dependent changes in the lifetime or anisotropy of DPH-PC, and thus that there are no pH-dependent structural changes within the DMPC bilayer, we wish to better understand the origin of the changes in the EPR spectra observed using 5-SASL. We have therefore also examined the frequency response of 2-AS in vesicles made from DMPC.

The parameters describing the intensity decay (using both the multiexponential and lifetime distribution model) for 2-AS as a function of pH and ionic strength are summarized in Table 5 and Fig. 6 *B*. The spectral parameters are all quite similar. There are no pH-dependent changes in $\langle\tau\rangle$ at 30°C. We do, however, observe a statistically significant increase in $\langle\tau\rangle$ at 50°C on raising the pH from 3.4 to 7.0, irrespective of the model used to describe the data. The temperature-dependent change in the pH-dependence of the measured lifetime is statistically significant as evidenced by force fitting the two component decay parameters to data taken at an alternative pH. For example, if the data taken at pH 7.0 is force fit with the two-component parameters taken from the data at pH 3.4, the χ^2_R values increase by a factor of 1.06 at 30°C, but 14.2-fold at 50°C (Table 5). There is no statistically significant effect of ionic strength on the mean decay time of 2-AS at 50°C, as judged by the modest increase in χ^2_R upon force fitting the parameters obtained from the low ionic strength conditions to the data obtained at the high ionic strength.

Anisotropy decays of 2-AS

The differential polarized phase angles and modulated anisotropy of 2-AS in DMPC were measured as a function of pH and ionic strength. Like DPH-PC either (*a*) a three correlation time model or (*b*) a two correlation time model involving motional restriction is required (data not shown). These are essentially equivalent models since θ_3 floats to a large number in model *a*. The approximately two-fold reduction in χ^2_R relative to the two-correlation time model indicates that the two-correlation time model with motional restriction is required with >99% confidence.

We note the similar correlation times obtained using 2-AS and DPH-PC (Table 4 and 6), further suggesting a physical basis for relating these correlation times to specific models describing lipid mobility (see above). The small increase in the correlation times for 2-AS relative to DPH-PC may be related to the position of the anthroate fluorophore closer to the membrane surface.

The frequency-domain data relating to the effect of pH and ionic strength on the rotational mobility of 2-AS are summarized in Table 6. At 30°C we observe that there is a reduction in both the correlation times and

TABLE 5 Multiexponential analysis of 2-AS in DMPC

Sample	$\langle\tau\rangle$	τ_1	α_1	τ_2	α_2	χ^{2a}_R
	ns	*ns*		*ns*		
30°C						
pH 3.4	7.84	2.14	0.24	8.32	0.76	1.60 (8.1)[a]
pH 7.0	7.84	2.78	0.25	8.39	0.75	0.76 (5.6)
pH 9.0	7.87	2.64	0.28	8.54	0.72	1.16 (8.3)
pH 7.0/pH 3.4[b]						0.81
pH 9.0/pH 3.4						1.04
50°C						
pH 3.4	4.89	0.73	0.22	5.06	0.78	1.46 (11.0)
pH 7.0	5.26	0.85	0.16	5.40	0.84	1.33 (7.2)
pH 9.0	5.25	0.78	0.17	5.38	0.83	1.18 (7.6)
pH 7.0/pH 3.4						18.9
pH 9.0/pH 3.4						19.0
50°C; 1.0 M KCl:						
pH 3.4	5.03	0.46	0.26	5.17	0.74	1.2 (6.8)
pH 7.0	5.25	0.21	0.31	5.34	0.69	1.3 (4.7)
pH 9.0	5.35	0.72	0.18	5.49	0.82	1.5 (6.2)
pH 3.4; no salt/pH 3.4: 1.0 M KCl M KCl						2.3
pH 7.0; no salt/pH 7.0: 1.0 M KCl M KCl						1.4
pH 9.0; no salt/pH 9.0: 1.0 M KCl M KCl						1.9

[a]The bracketed number corresponds to the χ^2_R for the single exponential fit to the data. Standard deviation of $\langle\tau\rangle$ is ±0.1 ns, where the error in the phase and modulation measurements typically are 0.2 degrees and 0.01, respectively. [b]The data from the first listed sample (before slash) were force fit with the parameters from the fit for the second listed sample (after slash).

TABLE 6 Anisotropy decay parameters for 2-AS in dimyristoylphosphatidylcholine as a function of pH, temperature, and ionic strength

Sample[a]	$\langle\tau\rangle$	θ_1	θ_2	g_1	g_2	r_∞	χ^2_R
	ns	*ns*	*ns*				
30°C							
pH 3.4	7.84	0.39	5.9	0.36	0.46	0.047	3.9 (5.8)[b]
pH 7.0	7.84	0.27	4.4	0.36	0.50	0.035	1.4 (4.1)
pH 9.0	7.87	0.25	4.7	0.34	0.52	0.034	3.4 (6.7)
pH 7.0/pH 3.4[c]							9.0
pH 9.0/pH 3.4							8.1
50°C							
pH 3.4	4.89	0.29	3.1	0.53	0.36	0.027	1.5 (1.7)
pH 7.0	5.26	0.25	2.5	0.48	0.41	0.027	2.4 (4.0)
pH 9.0	5.25	0.29	2.9	0.50	0.40	0.027	1.2 (2.5)
pH 7.0/pH 3.4							2.5
pH 9.0/pH 3.4							1.9
50°C; 1.0 M KCl:							
pH 3.4	5.03	0.30	2.9	0.44	0.43	0.033	0.30 (2.1)
pH 7.0	5.25	0.28	3.5	0.52	0.39	0.023	0.75 (9.8)
pH 9.0	5.35	0.24	2.3	0.45	0.44	0.031	0.83 (3.2)
pH 3.4; no salt/pH 3.4: 1.0 M KCl							4.9
pH 7.0; no salt/pH 7.0: 1.0 M KCl							2.1
pH 9.0; no salt/pH 9.0: 1.0 M KCl							0.9

[a]The standard errors are calculated from the least squares fit to the data, and are typically ±25% for θ_1; ±20% for θ_2; ±11% for g_1; ±8% for g_2; ±21% for r_∞. [b]The bracketed number corresponds to the χ^2_R for the 2 correlation time model. [c]The data from the first listed sample (before slash) were force fit with the parameters from the fit for the second listed sample (after slash). Standard errors for the phase and modulation measurements were 0.2 degrees and 0.02, respectively. r_o was determined to be 0.259 from steady state measurements of 2-AS in propylene glycol at −60°C (see Eq. 2 in Methods).

residual anisotropy upon increasing the pH from 3.4 to 7.0. Under these conditions there is no pH-dependent change in $\langle\tau\rangle$, indicating that the pH-dependent spectral changes observed using stearic-acid spin labels most probably involve an alteration in the mobility, but not a change in the polarity of the probe.

On the other hand at 50°C the anisotropy of 2AS is not dependent on the pH or ionic strength (at least pH 7 and 9), as determined by force fitting the parameters from the two correlation time model involving motional restriction (2θ, r_∞) to data sets acquired at the alternative pH and ionic strength. The insensitivity of 2AS to changes in ionic strength, in comparison to DPH-PC or 5-SASL, may be related to the transition moment of the anthroyl chromophore which need not be parallel to the membrane normal, and is therefore not simply related to the order parameter of the fatty acyl chains.

DISCUSSION

Multicomponent spectra have been observed utilizing stearic-acid spin labels in phosphatidylcholine vesicles at pH 7.2 that have been interpreted as arising from multiple ionization states of the stearic acid. This interpretation, if it is correct, would considerably complicate both the detection of membrane structural heterogeneity and the utilization of physical models that have been directed toward quantitatively understanding both the EPR spectra and the physical significance of the correlation times and residual anisotropy obtained from fluorescence data. Therefore, in an effort to evaluate the limitations inherent in the use of fatty acid probes to detect membrane structural changes we have measured directly the relaxation properties and dynamics of spin-labeled and anthroyloxy derivatives of stearic acid in phosphatidylcholine vesicles. By comparing these spectroscopic derivatives of stearic acid with a phospholipid analogue (i.e., DPH-PC) as a function of pH, ionic strength, and temperature we have been able to discriminate between spectral effects originating from the ionization of the α-carbonyl on the stearic acid and those originating from membrane structural changes.

Ionization state of spin-labeled and anthroyloxy derivatives of stearic acid

Upon titrating the hydrogen ion concentration we resolve a two-component spectrum for 5-SASL (at 50°C), indicating a heterogeneous degree of ionization with a pK_a near 6.3 (Fig. 3 and Table 1). Likewise, there are pH-dependent changes in the lifetime (or dynamics) of 2-AS between pH 3.4 and 7.0, but not between pH 7.0 and 9.0 (Fig. 6, Tables 5 and 6; see below), indicating that the α-carbonyl group of these stearic acid labels are essentially fully ionized at pH 7.0. The pH-dependent spectral changes of these fatty acid analogues arise as a result of their state of ionization, rather than from structural changes of the bilayer, as demonstrated by the observation that there are no pH-dependent changes in the lifetime or dynamics of the phospholipid analogue DPH-PC (which has no titratable residues over this pH range; Tables 2 and 4). The general agreement obtained between spin labeled and fluorescently labeled stearic acid analogues, using different phospholipid concentrations and vesicle preparations (i.e., large multilamellar vs. small unilamellar) provides confidence that these fatty acid probes remain essentially fully ionized at pH 7.0 over a broad range of conditions, and therefore these spectroscopic probes accurately reflect both temperature and ionic-strength induced alterations in the structure and conformational heterogeneity of biological membranes (see below).

Temperature-dependent changes in the bilayer structure

The spectra obtained using stearic acid spin labels at 30°C are characteristic of a single-component, independent of the degree of ionization of the stearic acid label (Fig. 3, *inset*). Likewise, the lifetime of the anthroyloxy stearic acid label is independent of pH. These results indicate that at 30°C the position of the fluorophore relative to the membrane surface is unaltered by the degree of ionization of the α-carbonyl group, since polarity differs significantly at each acyl chain position (Griffith et al., 1974). We do, however, observe a pH-dependent increase in the rotational mobility of the 2-AS label above the pK_a at 30°C (Table 6), that may be related to changes in hydrogen bonding between the protonated α-carbonyl of the probe and the phospholipid's headgroup. This is consistent with the progressive increase observed in the outer splitting ($T_\parallel'$) of the spin-label EPR spectra with increasing pH, since a greater mobility associated with the deprotonated α-carbonyl group would facilitate hydrogen-bonding between the nitroxide and the surrounding solvent, resulting in a larger outer splitting (Gagua et al., 1978; reviewed by Marsh, 1981).

On the other hand, at 50°C we observe a pH-dependent increase in the lifetime of 2-AS, but no significant change in the probe's rotational dynamics. Therefore at 50°C the lifetime, and thus the fluorophore's polarity, is dependent on the ionization state of the α-carbonyl group on the stearic acid probe. This is in

agreement with the spin-label EPR results in which two spectral components are resolved near the pK_a (i.e., two distinct environments are observed), as a result of the much larger polarity gradient at 50°C relative to 30°C.

The relationship between the spectral properties of both anthroate and nitroxide stearic acid analogues and the ionization state of the α-carbonyl group are thus very different at 30°C and 50°C, indicating a significant temperature-dependent alteration in the membrane structure. This probably involves a change in the mean conformation of the phosphatidylcholine headgroup (and thus the dipole moment between the phosphate and choline moieties relative to the membrane surface). In general, under physiological temperatures and ionic strengths, the phosphatidylcholine headgroup (and associated dipole) is thought to lie nearly parallel to the plane of the membrane (reviewed by Gennis, 1989). Under these conditions the α-carbonyl on the stearic acid spin label would lie at the same position relative to the membrane normal whether protonated, and interacting more strongly with phosphate groups, or unprotonated and interacting more strongly with the choline groups; consistent with the data obtained at 30°C. The appearance of multicomponent spectra near the pKa of the stearic acid spin label at 50°C (Fig. 3 *B*) is associated with a temperature-dependent change in the mean conformation of the phosphatidylcholine headgroup so that the position of the α-carbonyl on the stearic acid spin label is dependent on its state of protonation (i.e., the associated dipole no longer lies strictly parallel to the membrane surface). We emphasize that the appearance of spectral heterogeneity near the pKa is not indicative of any phospholipid structural heterogeneity, rather that the conformation of the headgroup has changed. Likewise, these results are inconsistent with proton exchange at the α-carbonyl on the stearic acid spin labels.

Ionic strength induced appearance of membrane structural heterogeneity

In agreement with previous work we find that under certain conditions (e.g., 50°C, neutral pH, and high ionic strengths) multicomponent spectra are observed for 5-SASL in phosphatidylcholine vesicles (Barratt and Laggner, 1974; Sanson et al., 1976; Egret-Charlier et al., 1978). This does not arise as a result of heterogeneity in the degree of ionization of the label as had been previously suggested, since stearic acid spin labels are essentially fully ionized at neutral pH (see above). Furthermore, increasing the ionic strength stabilizes the deprotonated form of the fatty acid (i.e., decreases the pK_a; Egret-Charlier et al., 1978; Ptak et al., 1980), resulting in an even more homogeneous population of fully ionized fatty acids. Finally, the lifetime and rotational mobility of the phospholipid derivative DPH-PC (with no ionizable group over this pH range) also decreases upon raising the ionic strength (independent of the pH) emphasizing that the ionic strength is affecting the phospholipid structural properties. The results are consistent with ^{2}H-NMR measurements that indicate the phospholipid's headgroup orientation relative to the membrane surface to be very sensitive to the charge of the bilayer (Seelig, 1987). However, ^{2}H-NMR spectra always give rise to a single quadrupole splitting, indicating a single time-averaged headgroup conformation on the microsecond time-scale. The orientational resolution and faster time-scale of the spin-label EPR technique permits the resolution of the ionic-strength induced structural heterogeneity. The physical basis for the observed structural heterogeneity at higher ionic strengths is unclear at present. The higher ionic strength may disrupt electrostatic interaction between phospholipid headgroups, where the resulting increase in conformational heterogeneity may allow a closer juxtaposition, and a corresponding increase in the hydrocarbon chain packing (i.e., motional anisotropy). Likewise, osmotic gradients may be relevant to the ionic strength-dependent effects (Mayer et al., 1985; Gruner et al., 1985). In any case, the resolution of the spectral heterogeneity using 5-SASL (Fig. 2) indicates the presence of membrane structural heterogeneity in single component model membranes composed of dimyristoyl phosphatidylcholine, and provides the first evidence for phospholipid headgroup structural heterogeneity under physiological (i.e., hydrated) conditions. The observed structural heterogeneity may be related to previous observations of multiple phosphatidylcholine headgroup conformations observed by x-ray and neutron diffraction (Pearson and Pascher, 1979; Hauser et al., 1981), but these latter measurements involve partially dehydrated samples and may not reflect normal headgroup conformations.

Conclusions

We have detected temperature-dependent and ionic-strength induced structural changes in single component model membranes that are probably related to the conformation and/or dynamics of the phosphatidylcholine headgroup in DMPC. These results should be applicable to other acyl chain compositions, since in general the acyl chain portion of the phospholipid does not significantly influence the headgroup's dynamics (Seelig and Seelig, 1980). While the physiological significance of these membrane structural changes remain to be investigated, we note that changes in the dipolar moment of phosphatidylcholine headgroups relative to the membrane normal may be sufficient to modulate the

structure and function of membrane associated proteins (Honig et al., 1986; Seelig et al., 1987). Furthermore, transient increases in ionic concentrations or gradients occur in a number of biologically significant responses (e.g., excitation-contraction coupling), and these ionic gradients may induce an alteration in the phospholipid's headgroup conformation which in turn could modulate voltage-dependent channel proteins. Therefore, further studies will be directed toward both clarifying the origins of structural heterogeneity in these simple model membrane systems and investigating lipid structural diversity in biological membranes.

Supported by grant GM-35719 (Dr. Lai) from the National Institutes of Health, an NIH postdoctoral fellowship GM-12814 (Dr. Squier); and a biotechnology fellowship from the National Biomedical ESR Center (Dr. Squier and Dr. Mahaney). This work was performed with the facilities at the Center for Fluorescence Spectroscopy (National Science Foundation DIR 8710401) and the National Biomedical ESR Center (RR01-008).

Received for publication 13 June 1990 and in final form 19 November 1990.

REFERENCES

Alcala, J. R., E. Gratton, and F. G. Prendergast. 1987. Resolvability of fluorescence lifetime distributions using phase fluorometry. *Biophys. J.* 51:587–596.

Barratt, M., and P. Laggner. 1974. The pH-dependence of esr spectra from nitroxide probes in lecithin dispersions. *Biochim. Biophys. Acta.* 363:127–133.

Bigelow, D. J., and D. D. Thomas. 1987. Rotational dynamics of lipid and the Ca-ATPase in sarcoplasmic reticulum. *J. Biol. Chem.* 262:13449–13456.

Bocian, D. F., and S. I. Chan. 1978. NMR studies of membrane structure and dynamics. *Annu. Rev. Phys. Chem.* 29:307–335.

Cevc, G., A. Watts, and D. Marsh. 1981. Titration of the phase transition of phosphatidylserine bilayer membranes. Effects of pH, surface electrostatics, ion binding, and headgroup hydration. *Biochemistry.* 20:4955–4965.

Davoust, J., M. Seigneuret, P. Herve, and P. F. Devaux. 1983. Collisions between nitrogen-14 and nitrogen-15 spin-labels. 2. Investigations on the specificity of the lipid environment of rhodopsin. *Biochemistry.* 22:3146–3151.

Deese, A. J., and E. A. Dratz. 1986. Carbon-13 and proton nmr studies of the interactions of lipids with membrane proteins. *In* Progress in Protein-Lipid Interactions. A. Watts and J. J. H. H. M. De Pont, editors. Elsevier Science Publishers, Netherlands. 2:45–82.

Egret-Charlier, M., A. Sanson, and M. Ptak. 1978. Ionization of fatty acids at the lipid-water interface. *FEBS (Fed. Eur. Biochem. Soc.) Lett.* 89:313–316.

Eisinger, J., and J. Flores. 1983. Cytosol-membrane interface of human erythrocytes. A resonance energy transfer study. *Biophys. J.* 41:367–379.

Ellena, J. F., S. J. Archer, R. N. Dominey, B. D. Hill, and D. S. Cafiso. 1988. Localizing the nitroxide group of fatty acid and voltage-sensitive spin-labels in phospholipid bilayers. *Biochim. Biophys. Acta.* 940:63–70.

Engel, L. W., and F. G. Prendergast. 1981. Values for and significance of order parameters and "cone angles" of fluorophore rotation in lipid bilayers. *Biochemistry.* 20:7338–7345.

Esmann, M., and D. Marsh. 1985. Spin-label studies on the specificity of lipid-protein interactions in Na^+, K^+-ATPase membranes from *Squalus acanthias*. *Biochemistry.* 24:3572–3578.

Esmann, M., K. Hideg, and D. Marsh. 1988. Novel spin-labels for the study of lipid-protein interactions. Application to (Na^+, K^+)-ATPase membranes. *Biochemistry.* 27:3913–3917.

Fajer, P., D. D. Thomas, J. B. Feix, and J. S. Hyde. 1986. Measurement of rotational motion by time-resolved saturation transfer electron paramagnetic resonance. *Biophys. J.* 50:1195–1202.

Faucon, J. F., and J. R. Lakowicz. 1987. Anisotropy decay of diphenylhexatriene in melittin-phospholipid complexes by multifrequency phas-modulation fluorometry. *Arch. Biochem. Biophys.* 252: 245–258.

Feix, J. B., C. A. Popp, S. D. Venkataramu, A. H. Beth, J. H. Park, and J. S. Hyde. 1984. An electron-electron double-resonance study of interactions between [^{14}N]- and [^{15}N] stearic acid spin label pairs: Lateral diffusion and verticle fluctuations in dimyristoyl phosphatidyl choline. *Biochemistry.* 23:2293–2299.

Feix, J. B., J. J. Yin, and J. S. Hyde. 1987. Interactions of ^{14}N:^{15}N stearic acid spin-label pairs: effects of host lipid alkyl chain length and unsaturation. *Biochemistry.* 26:3850–3855.

Flewelling, R. F., and W. L. Hubbell. 1986. The membrane dipole potential in a total membrane potential model: application to hydrophobic ion interactions with membranes. *Biophys. J.* 49:541–552.

Gaffney, B. J. 1976. Practical considerations for the calculation of order parameters for fatty acid or phospholipid spin labels in membranes. *In* Spin Labeling, Theory and Applications. L. J. Berliner, editor. Academic Press, New York. 567–571.

Gaffney, B. J., and D. C. Lin. 1976. Spin-label measurements of membrane-bound enzymes. *In* The Enzymes of Biological Membranes. Physical Chemical Techniques. 1:71–90.

Gagua, A. V., G. G. Malenkov, and V. P. Timofeev. 1978. Hydrogen bond contribution to the isotropic hyperfine splitting constant of a nitroxide free radical. *Chem. Phys. Lett.* 56:470–473.

Gennis, R. B. 1989. Biomembranes: Molecular Structure and Function. Springer-Verlag, New York.

Godici, P., and F. R. Landsberger. 1974. The dynamic structure of lipid membranes. A ^{13}C nuclear magnetic resonance study using spin labels. *Biochemistry.* 13:362–368.

Griffith, O. H., and P. C. Jost. 1976. Lipid spin labels in biological membranes. *In* Spin Labeling, Theory and Applications. L. J. Berliner, editor. Academic Press Inc. New York. 454–523.

Griffith, O. H., P. J. Dehlinger, and S. P. Van. 1974. Shape of the hydrophobic barrier of phospholipid bilayers: evidence for water penetration in biological membranes. *J. Membr. Biol.* 15:159–192.

Gruner, S. M., R. P. Lenk, A. S. Janoff, and M. J. Ostro. 1985. Novel multilayered lipid vesicles: comparison of physical characteristics of multilamellar liposomes and stable plurilamellar vesicles. *Biochemistry.* 24:2833–2842.

Hauser, H., A. Drake, and M. C. Phillips. 1976. Ion-binding to phospholipids. Interaction of calcium with phosphatidylserine. *Eur. J. Biochem.* 62:335–344.

Hauser, H., W. Guyer, and K. Howell. 1979. Lateral distribution of negatively charged lipids in lecithin membranes. Clustering of fatty acids. *Biochemistry.* 18:3285–3291.

Hauser, H., I. Pascher, R. H. Pearson, and S. Sundell. 1981. Preferred conformation and molecular packing of phosphatidylethanolamine and phosphatidylcholine. *Biochim. Biophys. Acta.* 650:21–51.

Honig, B. H., W. L. Hubbell, and R. F. Flewelling. 1986. Electrostatic interactions in membranes and proteins. *Ann. Rev. Biophys. Biophys. Chem.* 15:163–193.

Hubbell, W. I., and H. M. McConnell. 1971. Molecular motion in spin-labeled phospholipid membranes. *J. Am. Chem. Soc.* 93:314–326.

Joseph, J., and C.-S. Lai. 1988. Synthesis of a spin-labeled phospholipid for studying membrane dynamics in intact mammalian cells. *J. Lipid Res.* 29:1101–1104.

Jost, P. C., and O. H. Griffith. 1978*a*. The spin-labeling technique. *In* Methods in Enzymology. Enzyme Structure, part G. C. H. W. Hirs and S. N. Timasheff, editors. Academic Press, New York. 369–418.

Keith, A., D. Horvat, and W. Snipes. 1974. Spectral characteristics of ^{15}N spin labels. *Chem. Phys. Lipids.* 13:49–62.

Kinosita, K., S. Kawato, and A. Ikegama. 1977. A theory of fluorescence polarization decay in membranes. *Biophys. J.* 20:289–305.

Lai, C.-S. 1982. Electron Spin Resonance (Specialist Periodical Report). The Royal Society of Chemistry, London. 7:313–339.

Lakowicz, J. R. 1983. Principles of Fluorescence Spectroscopy. Plenum Publishing Corp., New York.

Lakowicz, J. R. 1988. Fluorescence spectroscopy. Principles and applications to biological macromolecules. *In* New Comprehensive Biochemistry: Modern Physical Methods. L. van Deenen, editor. Elsevier Science Publishers, Netherlands. 1–26.

Lakowicz, J. R., F. G. Prendergast, and D. Hogen. 1979. Differential polarized phase fluorometric investigations of diphenylhexatriene in lipid bilayers. Quantitation of hindered depolarizing rotations. *Biochemistry.* 18:508–519.

Lakowicz, J. R., H. Cherek, B. P. Maliwal, and E. Gratton. 1985. Time-resolved fluorescence anisotropies of diphenylhexatriene and perylene in solvents and lipid bilayers obtained from multifrequency phase-modulation fluorometry. *Biochemistry.* 24:376–383.

Lakowicz, J. R., G. Laczko, I. Gryczynski, and H. Cherek. 1986*a*. Measurement of subnanosecond anisotropy decays of protein fluorescence using frequency-domain fluorometry. *J. Biol. Chem.* 261: 2240–2245.

Lakowicz, J. R., G. Laczko, and I. Gryczynski. 1986*b*. 2-GHz frequency domain fluorometer. *Rev. Sci. Instrum.* 57:2499–2506.

Lakowicz, J. R., H. Cherek, I. Gryczynski, N. Joshi, and M. L. Johnson. 1987*a*. Analysis of fluorescence decay kinetics measured in the frequency domain using distributions of decay times. *Biophys. Chem.* 28:35–50.

Lakowicz, J. R., M. L. Johnson, W. Wiczk, A. Bhat, and R. F. Steiner. 1987*b*. Resolution of a distribution of distances by fluorescence energy transfer and frequency domain fluorometry. *Chem. Phys. Lett.* 138:587–593.

Lakowicz, J. R., I. Gryczynski, H. C. Cheung, C. K. Wang, and M. L. Johnson. 1988*a*. Distance distributions in native and random-coil troponin I from frequency-domain measurements. *Biopolymers.* 27:821–830.

Lakowicz, J. R., G. Laczko, I. Gryczynski, H. Szmacinski, W. Wiczk, and M. L. Johnson. 1989. Frequency domain fluorescence spectroscopy; principles, biochemical applications and future developments. *Ber. Bunseng. Phys. Chem.* 93:316–327.

Lange, A., D. Marsh, K. H. Wassmer, P. Meier, and G. Kothe. 1985. Electron spin resonance study of phospholipid membranes employing a comprehensive line-shape model. *Biochemistry.* 24:4383–4392.

Lipari, G., and A. Szabo. 1980. Effect of librational motions on fluorescence depolarization and NMR relaxation in macromolecules and membranes. *Biophys. J.* 30:489–506.

Marsh, D. 1980. Molecular motion in phospholipid bilayers in the gel phase: long axis rotation. *Biochemistry.* 19:1632–1637.

Marsh, D. 1981. Electron spin resonance: spin labels. *In* Membrane Spectroscopy. E. Grell, editor. Springer-Verlag. 51–142.

Mayer, L. D., M. J. Hope, P. R. Cullis, and A. S. Janoff. 1985. Solute distributions and trapping efficiencies observed in freeze-thawed multilamellar vesicles. *Biochim. Biophys. Acta.* 817:193–196.

Meraldi, J. P., and J. Schlitter. 1981. A statistical mechanical treatment of fatty acyl chain order in phospholipid bilayers and correlation with experimental data. B. Diplamitoyl-3-*sn*-phosphatidylcholine. *Biochim. Biophys. Acta.* 645:193–210.

Moser, M., D. Marsh, P. Meier, K. Wassmer, and G. Kothe. 1989. Chain configuration and flexibility gradient in phospholipid membranes: comparison between spin-label electron spin resonance and deuteron nuclear magnetic resonance, and identification of new conformations. *Biophys. J.* 55:111–123.

Pearson, R. H., and I. Pascher. 1979. The molecular structure of lecithin dihydrate. *Nature (Lond.).* 281:499–501.

Popp, C. A., and J. S. Hyde. 1981. Effects of oxygen on epr spectra of nitroxide spin labeled probes in model membranes. *J. Magn. Reson.* 43:249–258.

Prendergast, F. G., R. P. Haugland, and P. J. Callahan. 1981. 1-(4-Trimethylamino-phenyl)-6-phenylhexa-1,3,5-triene: synthesis, fluorescence properties, and use as a fluorescence probe of lipid bilayers. *Biochemistry.* 20:7333–7338.

Ptak, M., M. Egret-Charlier, A. Sanson, and O. Bouloussa. 1980. An nmr study of the ionization of fatty acids, fatty amines, and *n*-acylamino acids incorporated into phosphatidylcholine vesicles. *Biochim. Biophys. Acta.* 600:387–397.

Rooney, E. K., J. M East, O. T. Jones, J. McWhirter, A. C. Simmonds, and A. G. Lee. 1983. Interaction of fatty acids with lipid bilayers. *Biochim. Biophys. Acta.* 728:159–170.

Sanson, A., M. Ptak, J. L. Rigaud, and C. M. Gary-Bobo. 1976. An esr study of the anchoring of spin-labeled stearic acid in lecithin multilayers. *Chem. Phys. Lipids.* 17:435–444.

Schachter, D., U. Cogan, and R. E. Abbott. 1982. Asymmetry of lipid dynamics in human erythrocyte membranes studied with permeant fluorophores. *Biochemistry.* 21:2146.

Scherer, J. R. 1989. On the position of the hydrophobic/hydrophilic boundary in lipid bilayers. *Biophys. J.* 55:957–964.

Seelig, J. 1970. Spin label studies of oriented smectic liquid crystals (a model system for biological membranes). *J. Am. Chem. Soc.* 92:3881–3887.

Seelig, A., and J. Seelig. 1974. The dynamic structure of fatty acyl chains in a phospholipid bilayer measured by deuterium magnetic resonance. *Biochemistry.* 13:4839–4845.

Seelig, S., and A. Seelig. 1980. Lipid conformation in model membranes and biological membranes. *Q. Rev. Biophys.* 13:19–61.

Seelig, J., P. M. Macdonald, and P. G. Scherer. 1987. Phospholipid head groups as sensors of electric charge in membranes. *Biochemistry.* 26:7535–7541.

Squier, T. C., and D. D. Thomas. 1989. Selective detection of the rotational dynamics of the protein associated lipid hydrocarbon chains in sarcoplasmic reticulum membranes. *Biophys. J.* 56:735–748.

Squier, T. C., D. J. Bigelow, and D. D. Thomas. 1988. Lipid fluidity directly modulates the overall protein rotational mobility of the

Ca-ATPase in sarcoplasmic reticulum. *J. Biol. Chem.* 263:9178–9186.

Taylor, M. G., and I. C. P. Smith. 1981. Reliability of nitroxide spin probes in reporting membrane properties: a comparison of nitroxide) and deuterium-labeled steroids. *Biochemistry.* 20:5252–5255.

Thomas, D. D. 1985. Saturation transfer EPR studies of microsecond rotational motions in biological membranes. *In* The Enzymes of Biological Membranes. 2nd ed. A. N. Martonosi, editor. Plenum Publishing Corp., New York. 1:287–312.

Thomas, D. D., T. M Eads, V. A. Barnett, K. M Lindahl, D. A. Momont, and T. C. Squier. 1985. Saturation transfer EPR and triplet anisotropy: complimentary techniques for the study of microsecond rotational dynamics. *In* Spectroscopy and the Dynamics of Molecular Biological Systems. P. M. Bayley and R. E. Dale, editors. Academic Press, Inc., New York. 239–257.

Thulburn, K. R., and W. H. Sawyer. 1978. Properties and locations of a set of fluorescent probes sensitive to the fluidity gradient of the lipid bilayer. *Biochim. Biophys. Acta.* 511:125–140.

Wendoloski, J. J., S. J. Kimatian, C. E. Schutt, and F. R. Salemme. 1989. Molecular dynamics simulation of a phospholipid micelle. *Science (Wash. DC).* 243:636–638.

Yin, J.-J., M. Pasenkiewicz-Gierula, and J. S. Hyde. 1987. Lateral diffusion of lipids in membranes by pulse saturation recovery electron spin resonance. *Proc. Natl. Acad. Sci. USA.* 84:964–968.

Yin, J.-J., J. B. Feix, and J. S. Hyde. 1988. Solution of the nitroxide spin-label spectral overlap problem using pulse electron spin resonance. *Biophys. J.* 53:525–531.